



ORIGINAL RESEARCH PAPER

Antibiofilm and antimicrobial efficacy evaluation of polypyrrole nanotubes embedded in aminated gum acacia based nanocomposite

Nathiya Dhananjayan¹  | Karthika Viswanathan² | Wilson Jeyaraj¹  |
Arumugam Ayyakannu² | Gurunathan Karuppasamy³

¹Department of Bioelectronics and Biosensors, Alagappa University, Karaikudi, India

²Department of Botany, Alagappa University, Karaikudi, India

³Department of Nanoscience and Technology, Alagappa University, Karaikudi, India

Correspondence

Wilson Jeyaraj, Department of Bioelectronics and Biosensors, Science Block, Alagappa University, Karaikudi, Sivaganga 630 004, Tamil Nadu, India. Email: wilson.j2008@yahoo.com

Funding information

Department of Higher Education, Grant/Award Number: RUSA 2.0 [F24-51/2014-U, Policy (TN Multi-Gen), Dept of Edn, Govt]; Science and Engineering Research Board, Grant/Award Number: EMR/2014/000010

Abstract

The sustainable development of natural polysaccharide-based hybrid composites is highly important for the effective replacement of metal nanoparticles in diverse applications. Here, polypyrrole nanotubes (PPyNTs) were embedded on the surface of aminated gum acacia (AGA) to produce ecofriendly nanocomposites for biomedical applications. The morphology of a PPyNT-enhanced AGA (PPyNT@AGA) hybrid nanocomposite was studied by scanning electron microscopy and transmission electron microscopy and their affirmed interactions were characterised by X-ray diffraction, Raman, Fourier transform-infrared and UV-visible spectroscopy. Interestingly, the prepared PPyNT@AGA nanocomposite exhibited 90% biofilm inhibition against gram-negative *Pseudomonas aeruginosa*, gram-positive *Streptococcus pneumoniae* and fungal strain *Candida albicans* with promising antimicrobial performance. This study establishes the good inhibition of a PPyNT@AGA hybrid composite against various microorganisms. The stability of the nanocomposite coupled with antimicrobial activity enables an effective strategy for diagnosing and controlling pathogens.

1 | INTRODUCTION

Among different conducting polymers, polypyrrole (PPy) has garnered much attention in biomedical application because of its easy preparation, high conductivity, good chemical stability, tunable electrical and optical property [1, 2]. PPy, a polycationic polymer, is reported to have excellent antimicrobial efficacy because of its pronounced biocompatibility and high stability [3]. It can easily be synthesised using various organic solvents and oxidative or chemical polymerisation methods at a neutral pH solution in an aqueous medium [4]. The strong intermolecular and intramolecular force in the PPy structure demonstrates colloidal solubility in an aqueous medium [5]. To address this issue, researchers attempted to synthesize PPy in different nanostructures such as nanospheres, nanowires,

nanotubes, and nanorods, confirming the modified physicochemical and electronic properties [6]. On the other hand, the high surface area of nanostructured PPy more often tends toward agglomeration because of Van der Waals forces, thus leading to instability [7]. To attain an agglomeration-free structure, the strategies employed in synthesis methods of PPy were the use of a hard template (using the porous form of aluminium oxide, silver or silica) and a soft template (using the surfactant of micelles). However, the structural property of PPy was modified using strong acids and more surfactants in hard and soft template methods, respectively [8, 9]. In another way, the stability of the nanostructured PPy was investigated by doping on or with carbon materials (reduced graphene oxide [10], multi walled carbon nanotube (MWCNT) [11], etc.), metal nanoparticles (NPs) (CuO [12],

This is an open access article under the terms of the Creative Commons Attribution-NonCommercial-NoDerivs License, which permits use and distribution in any medium, provided the original work is properly cited, the use is non-commercial and no modifications or adaptations are made.

© 2021 The Authors. *IET Nanobiotechnology* published by John Wiley & Sons Ltd on behalf of The Institution of Engineering and Technology.

Fe₃O₄ [13], Ag [14], etc.) and biomolecules (cellulose [15], chitosan [16], etc.) for biomedical applications. Among these, the hybrid composite formation of PPy with natural polysaccharides exhibited more biodegradability and biocompatible ability with enhanced stability and antimicrobial power and has attracted the attention of scientists in the biomedical field [2, 17].

Gum arabic (GA), a natural biopolymer, is composed of D-galactose (~40% of residues), L-arabinose (~24%), L-rhamnose (~13%), and two types of uronic acids responsible for the polyanionic character of the gum, D-glucuronic acid (~21%) and 4-O-methyl-D-glucuronic acid (~2%) [18, 19]. The wide abundance of GA in the Indian forest makes it an excellent candidate for food and pharmaceutical industries; it also possesses various physicochemical characteristics such as solubility, colloidal stability, ecofriendliness, and emulsifying, encapsulation and biosorption properties [20]. Bandyopadhyaya et al. [21] reported GA on the electrosteric stabilisation of carbon nanotubes (CNTs) by interroping the nanotubes with enhanced dispersibility. The use of GA-encapsulated hybrid composites was extended to biomedical applications owing to their soluble nature and antimicrobial and antibiofilm abilities [18, 22]. The antimicrobial and antibiofilm efficacy of the proposed composite is investigated in this work.

Moreover, progress in research on PPy nanotube (PPyNT)-based composites is widely applied in drug delivery, textile and sensing applications with antimicrobial and antioxidant efficacy [18, 22–25]. For example, Zhao et al. [26] studied the antibiotic resistance property of encapsulated NPs over linear polymers and reported that the multiple functional groups facilitate higher cell recognition and binding capabilities [27]. In other work, PPy anchored with palladium NPs and reduced graphene oxide exhibited good antibiofilm efficacy owing to its more reactive groups on the composite surface [28]. Similarly, a composite film based on GA/polyvinyl alcohol/chitosan incorporated with black pepper oil and ginger oil showed significant inhibition against microbes [20]. In addition, Murugesan et al [11] monitored the antibiofilm effect of MWCNT-supported Pd-doped PPy for a chemotherapeutic approach against cancer. Hence, the ability of resistance to microbial pathogenesis is considered to be the pivotal factor for therapeutic applications [2, 24]. Therefore, we designed aminated GA enhanced with PPyNTs for more facile interaction and disruption towards cell walls of microbial pathogens.

In this study, we demonstrate the physicochemical interaction of a PPyNT-enhanced aminated gum acacia (AGA) (PPyNT@AGA) nanocomposite and its antibiofilm and antimicrobial efficacy against different microbial pathogens. To the best of our knowledge, no report has discovered the potential antibiotic resistance property of PPyNT@AGA nanocomposites. We assessed the stability of the as-prepared PPyNT@AGA nanocomposite, conducted systematic material characterisation, and investigated its antibiofilm and antimicrobial effectiveness. We expect that our findings from the proposed composite will provide an alternative strategy for a

promising future in wound dressing and drug-delivery applications.

2 | EXPERIMENTAL SECTION

2.1 | Materials and collection of microbes

All chemicals used were of analytical grade used without further purification. Methyl orange (MO), ferric chloride (FeCl₃), pyrrole, GA, ethylene diamine, HCl, acetone, and microbial media were purchased from Himedia, Mumbai. Gram-positive and gram-negative bacteria, including *Staphylococcus aureus* (MTCC1935) *Streptococcus pneumoniae* (MTCC1936), *Klebsiella pneumoniae* (MTCC432), *Salmonella typhi* (MTCC3224), *Pseudomonas aeruginosa* (MTCC2642), and fungi *Candida albicans* (MTCC3959), were purchased from Microbial Type Culture Collection, India. For aqueous solutions, deionised (DI) water was used. Experiments were conducted at room temperature (~37°C).

2.2 | Material preparation and modification

2.2.1 | Preparation of PPyNTs

PPyNTs were synthesised by a simple oxidative polymerisation technique [28]. Briefly, 0.5 g of FeCl₃ and 5 mM of MO solution (60 ml) were stirred for 30 min, and then 210 µl of pyrrole monomer was slowly added into the solution over 10 min. The reaction mixture was maintained at –5°C for 36 h. After polymerisation, the black precipitate was filtered and purified with DI water and ethanol and then dried at 45°C for 12 h.

2.3 | Preparation of PPyNT-enhanced AGA nanocomposite

The PPyNT@AGA nanocomposite was prepared by a simple sol-gel method with amination and reduction using chemical agents of ethylenediamine (C₂H₈N₂) and HCl, respectively [29]. In brief, 1 g of GA powder was dissolved in 250 ml of DI water with stirring. Into that, 15 ml of C₂H₈N₂ was added to substitute the primary–OH groups of galactose and–COOH groups of glucuronic acid in GA with –NH₂CH₂CH₂NH₂, with stirring overnight. Into this colloidal solution, 100 mg of PPyNT was dispersed in 100 ml DI water using ultrasonication for 3 h. The colloidal solution of PPyNTs was added to the aminated GA reaction mixture with stirring for 5 h. Therefore, the –NH⁺ groups in PPyNTs electrostatically and electrosterically interacted with secondary –OH[–] groups in GA. Then, 1 M (50 ml) HCl was added for the reduction of –NH₂CH₂CH₂NH₂ into –NH₂ and stirred for 3 h (Figure 1). By mixing acetone with a sample solution at a ratio of 3:1, the modified polymer was separated and dried using a lyophiliser.

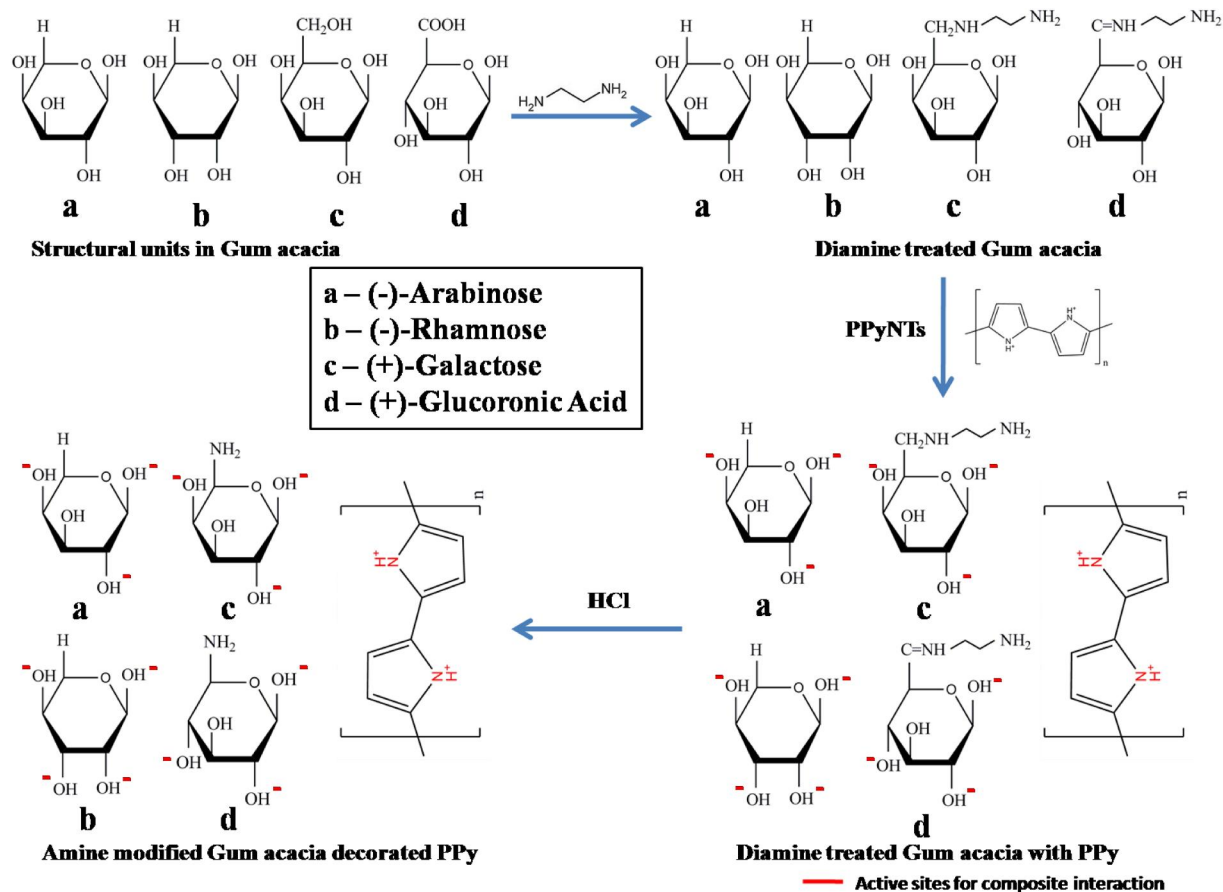


FIGURE 1 Schematic illustration of polypyrrole nanotube-enhanced aminated gum acacia composite in (a) antibiofilm and (b) antimicrobial

Similarly, AGA was synthesised separately by the sol-gel method for comparison purposes. Thus, the accumulated cationic functional groups in the prepared hybrid composite are very useful for facilitating more effective interaction towards a negatively charged cell membrane in microbial pathogens. Figure 2 shows a schematic illustration of a PPyNT@AGA composite in antibiofilm and antimicrobial studies.

2.4 | Characterisation

Scanning electron microscopy (SEM) images for PPyNTs, AGA and PPyNT@AGA nanocomposites were obtained using EVO 18 SEM (Carl Zeiss, Germany) operating at 21.00 kV. The transmission electron microscopy (TEM) image of the nanocomposite was obtained using a Tecnai G2 (F30) high-resolution transmission electron microscope. X-ray diffraction (XRD) patterns were obtained using a Bruker Germany D8 advance instrument ($\lambda = 1.5418 \text{ \AA}$) operated at 30 mA, 40 kV using Cu $k\alpha$ radiation. The Raman spectrum analysis was performed with an imaging spectrograph (model STR500 mm focal length) laser Raman spectrometer (SEKI Japan). The functional groups of the samples were further analysed using a Thermo Nicolet 200 FTIR spectrometer and

ALS-SEC2000 UV-vis spectrophotometer (Biologic). The antibiofilm activity of the PPyNT@AGA nanocomposite was studied by confocal laser scanning microscopy (CLSM) (Carl Zeiss LSM 710).

2.5 | Microbial assay

2.5.1 | Growth studies

Initially, the bacterial strains were cultured on tryptone soya agar plates, incubated at 37°C for 24 h, and stored at 4°C for further experiments [30]. *C. albicans* were cultured in yeast extract peptone dextrose medium (1% yeast extract, 2% peptone, 2% dextrose; Himedia Laboratories) by incubation at 37°C for 12 h at 160 rpm, and stored at 4°C for further experiments [31]. Before testing, the microbial cultures were subcultured at least twice and grown for 24 h at 37°C on agar plates. For growth studies, 10^6 cells (optical density $A_{600} = 0.1$) of test strains were grown aerobically in 50 ml media on an automated shaker set at 37°C with 200 rpm agitation. PPyNT@AGA nanocomposites with final concentrations of $0 \times$ minimum inhibitory concentration (MIC), $0.5 \times$ MIC and $1 \times$ MIC for each test were added to cultures. For the analysis of growth kinetics, bacterial cells (1×10^6)

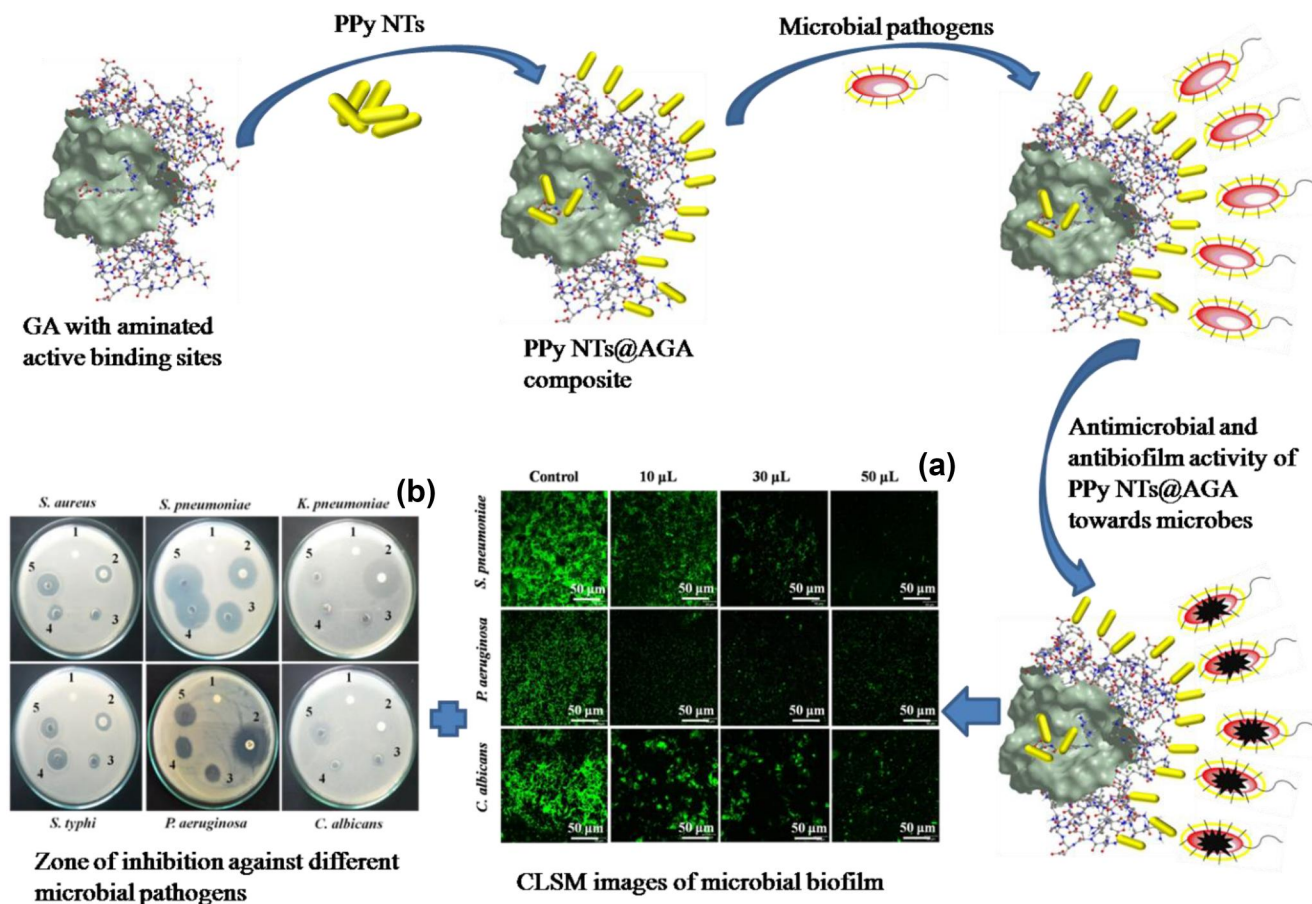


FIGURE 2 Structural illustration of amine modified gum acacia and its interaction with polypyrrole nanotubes

were inoculated in the PPyNT@AGA (10, 30, 50 and 100 µg/ml) at 37°C for 12 h using azithromycin as positive control. Similarly, fungal cells (3.2×10^7) were inoculated in the PPyNT@AGA (10, 30, 50 and 100 µg/ml) at 37°C for 12 h using fluconazole as positive control. Optical density (OD) values were taken at 1-h intervals for 24 h and the growth curve was plotted as OD_{600nm} against the time interval.

2.6 | Determination of minimum inhibitory concentrations of PPyNT-enhanced AGA

The MICs of PPyNT@AGA against fungal were examined using the microtiter plate method (CLSI, 2015) [32, 33]. In brief, 1% of an overnight culture of *S. aureus* (1×10^6) was inoculated in 200 µl of nutrient broth with different concentrations of PPyNT@AGA (0, 20, 40, 60, 80, 100, 120, 140, 160, 180 and 200 µg/ml) and incubated at 37°C for 24 h. In a similar way, bacterial cultures of *S. pneumoniae*, *K. pneumoniae*, *S. typhi*, and *P. aeruginosa* were prepared for MIC analysis with 20 µg/ml of azithromycin as positive control. For fungal analysis, 1% of an overnight culture of *C. albicans* (3.2×10^7) was allowed to grow in potato dextrose agar medium containing PPyNT@AGA in varying concentrations (0

to 200 µg/ml) with 20 µg/ml of fluconazole as positive control. After incubation, the cell density of the bacterial and fungal cultures was measured at 600 nm using SpectraMax M3 (Molecular Devices).

2.7 | Well-diffusion assay

The antimicrobial activity of the prepared samples was investigated using the well-diffusion method [34]. The gram-positive (*S. aureus* and *S. pneumoniae*) and gram-negative (*K. pneumoniae*, *S. typhi*, and *P. aeruginosa*) bacteria were grown in nutrient agar medium and incubated at 37°C for 24 h followed by frequent subculture to fresh medium and were used as test bacteria. The fungal culture of *C. albicans* was grown in potato dextrose agar medium incubated at 37°C for 72 h followed by periodic subculturing in fresh medium and used as test fungi. Sterile Muller Hinton agar plates with 6-mm-diameter wells were used for culture. Then 0.1% overnight inoculums of *S. aureus*, *S. pneumoniae*, *K. pneumoniae*, *S. typhi*, *P. aeruginosa* and *C. albicans* were swabbed uniformly over the surface of Muller Hinton agar plates. To evaluate the antimicrobial potential of PPyNT@AGA, dimethylsulfoxide (DMSO)-dissolved GA, AGA, PPyNT and nanocomposite were added

to the wells, in which the solvent DMSO (100 μl) served as negative control and azithromycin (bacteria) and fluconazole (fungi) as positive control. In brief, the wells of a 96-well plate filled with bacterial suspension (1×10^6 colony-forming units ml^{-1}) and fungal suspension (3.2×10^7) were shake-incubated with increasing concentrations of PPyNT@AGA (0, 20, 40, 60, 80, 100, 120, 140, 160, 180 and 200 $\mu\text{g}/\text{ml}$) for 24 h at 37°C. All experiments were repeated thrice and the average values were presented.

2.7.1 | Biofilm assay

For antibiofilm screening, sterilised glass slides (1×1 cm) were placed in 24-well polystyrene plates loaded with 1.5 ml nutrient broth in each well. Lag phase bacterial cultures (*S. pneumoniae* and *P. aeruginosa*) with an OD value of 0.1 at 660 nm ($\sim 1 \times 10^9$ cells/ml) were used as inoculums and the plates were incubated at 37°C (pH 7.0) for 24 h. The 3-day fungal culture (*C. albicans*) diluted to the final concentration was 3.2×10^7 cells, which was counted using a haemocytometer (Neubauer Chamber, Merck) and incubated at 37°C (pH 7.0) for 24 h. After incubation, the PPyNT@AGA nanocomposite at different concentration was loaded into each well and incubated again for another 24 h at 37°C. The biofilm cells were stained by 0.1% crystal violet (Sigma Aldrich) followed by destaining with 10% glacial acetic acid. The absorbance of the solution was measured at 570 nm using a SpectraMax 3. All experiments were repeated thrice. The percentage of biofilm inhibition was calculated using the formula:

$$\% \text{ inhibition} = \frac{[(\text{control OD}_{570 \text{ nm}} - \text{treated OD}_{570 \text{ nm}})]}{\text{control OD}_{570 \text{ nm}}} \times 100.$$

To visualize the biofilm, glass slides were washed and stained with 0.1% acridine orange for 15 min, removing excess stain. Then, the glass slides were air-dried and observed under CLSM [31, 35].

2.8 | Statistical analysis

Antimicrobial and antibiofilm activities were analysed using analysis of variance followed by Duncan post hoc test. A *p* value of .05 was used as a threshold to assess significant differences among mean values of antimicrobial data and are shown as mean \pm standard deviation.

3 | RESULTS AND DISCUSSION

3.1 | Material characterisation

The XRD patterns of as-prepared samples of PPyNTs, AGA and PPyNT@AGA are shown in Figure 3(a). In PPyNTs, it showed small characteristics peaks at 2θ of 18.5°, 29.4°, and 34.3° owing to the nanostructured and semicrystalline nature of PPyNTs arising from π - π interaction in polymer chain [12]. AGA showed a wide maxima diffraction peak at 2θ of 20.2°,

representing an amorphous phase of biopolymer. The rise in intensity and broad diffraction peak in the PPyNT@AGA nanocomposite indicate the modification in the PPyNT semicrystalline nature caused by its strong adsorption with the AGA surface.

Figure 3(b) shows the Raman spectra of the prepared samples. In the PPyNT spectra, the main characteristic bands at 1552 cm^{-1} (C=C stretching vibrations of polymer backbone) and two bands of ring stretching at 1381 cm^{-1} and 1295 cm^{-1} are recorded [36]. In the composite, observation of individual bands of PPyNTs in PPyNT@AGA confirmed the feasible composite formation. Hong et al. [37] found the upshifting in symmetric C=C stretching mode of PPy and concluded that there was a distortion in the polymer causing a reduction in the polymer aromatic ring and π -conjugation length. Here, we noted an upshift of the C=C stretching band from 1552 to 1595 cm^{-1} ; it revealed the increased surface caused by a reduction in π -conjugation length of PPyNTs while it was combined with AGA. Marakova et al. [28] reported variations in Raman spectra intensity resulting from deprotonation caused from silver NP deposition with PPy. Hence, the increase in intensity and upshifting of the main band of PPyNT@AGA compared with PPyNTs signifies strong interaction in the synthesised nanocomposite.

The surface morphology of the as-prepared samples was observed from field emission-SEM images, as shown in Figure 2. As shown in Figure 2(a), the synthesised AGA had a fibrous morphology with fine pores with an average size of 0.29 μm . Figure 2(b) confirms that the PPyNTs were homogeneously and densely dispersed throughout the active surface of the AGA microstructure. Furthermore, we evidenced the tubular form of PPyNTs in the nanocomposite, which elucidates the formation of nanostructures. Williams et al. [38] reported the synergistic effect of surface charges in GA responsible for steric attraction towards magnetic NPs. Here, we speculate that the functionalised amine charges of AGA with carboxyl groups provided steric hindrance and bridged the PPyNTs. Thus, it maintained the steric separation of PPyNTs by hydrophilic and hydrophobic forces from AGA and resulted in agglomeration-free nanocomposite. In addition, the TEM image of the nanocomposite (Figure 4c) shows the adsorption of PPyNTs on the surface and in the pores of AGA. The respective selected area electron diffraction pattern further demonstrates the firm interaction of nanocomposite from the presence of diffraction rings which are in agreement with plane values observed in the XRD of PPyNTs (Figure 4d).

The dispersibility of PPyNTs with AGA in DI water is explored in Figure 5. For the successful validation of our work, the homogeneous solution was left to stand for 3 months and checked periodically. After it was left for 2 days, PPyNTs without AGA composite started to subside to the bottom of the solution, whereas with AGA it showed a well-dispersed composite, indicating good dispersibility with stability provided by AGA to the PPyNT nanocomposite in water. The experiment was consecutively checked after 5, 10, 20, 30, 60 and 90 days for long-term dispersibility. After 3 months of evaluation, the PPyNT colloidal solution with AGA maintained

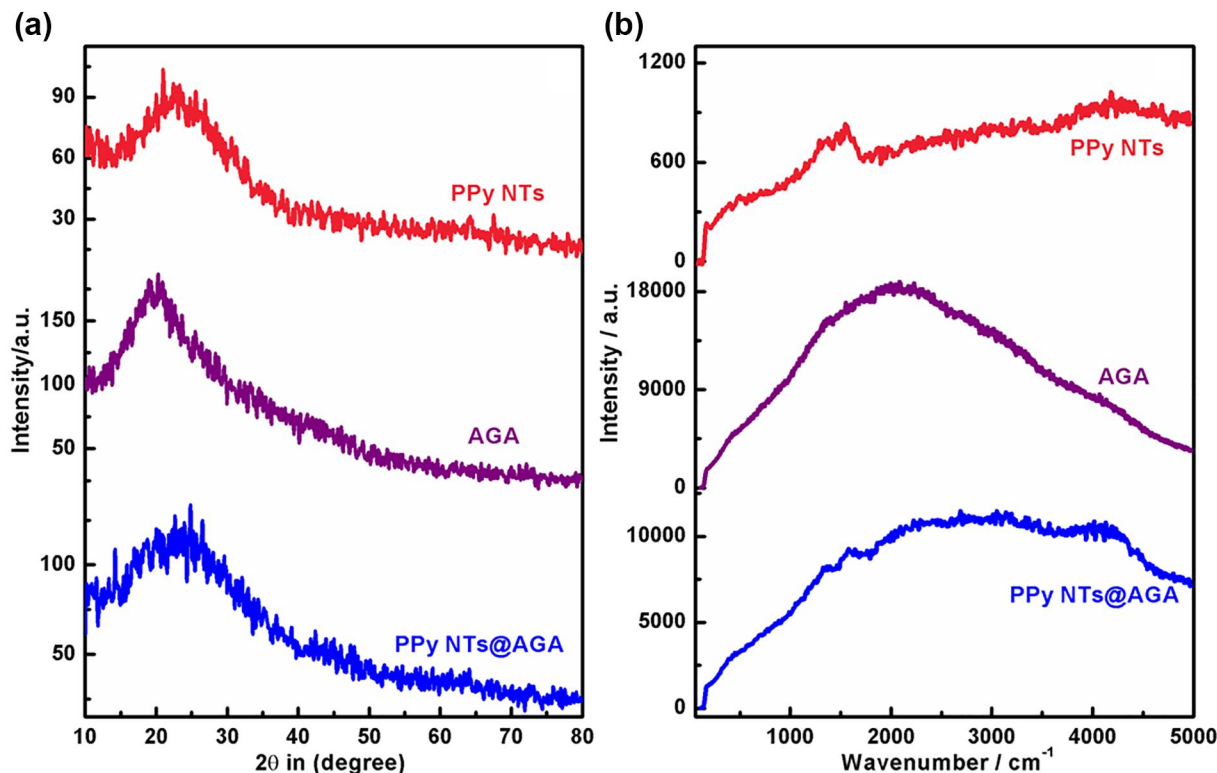


FIGURE 3 X-ray diffraction and Raman spectrum of (a) polypyrrole nanotube, (b) aminated gum acacia, (c) polypyrrole nanotube-enhanced aminated gum acacia nanocomposite

homogeneity, confirming the remarkable dispersibility of the nanocomposite owing to strong electrosteric and hydrophobic–hydrophilic interactions.

The presence of amine, alkyl and hydroxyl groups in PPyNTs and AGA is demonstrated by a Fourier transform-infrared study as shown in Figure 6(a). In Curve a, peaks at 1560 , 1420 and 1060 cm^{-1} are attributed to C–C stretching, C–N stretching and aliphatic C–N stretching vibrations of the pyrrole ring, respectively [28]. The observed main characteristic peaks at 1040 and 1350 cm^{-1} (C–O stretch), 1600 cm^{-1} (C=O stretch and N–H bending), and 2700 – 3600 cm^{-1} (O–H stretch) signify amine modification in the GA structure (Curve b) [25]. Upon modification of hydroxyl groups of GA to the $-\text{NH}_2$ group, the broad absorption band around 3500 shifted to 3600 cm^{-1} in AGA, confirming amine modification; this is supported in Figure S1. The presence of main characteristic peaks of PPyNTs were observed in the PPyNT@AGA nanocomposite (Curve c) with slightly shifted peak intensities and bands denoting changes in π -interactions of the prepared hybrid composite. Also, the wide band observed in AGA became sharper and shifted from 3140 to 3450 cm^{-1} in the nanocomposite; this was ascribed the reduction in $-\text{OH}$ groups owing to adsorbed $-\text{NH}$ groups from PPyNTs.

Further confirmation of successful hybrid composite formation was achieved from UV-Vis spectra analysis of as-prepared samples (Figure 6b). In Curve a, the absorption peak at 280 nm corresponds to π – π^* transition of the pyrrole aromatic ring [10]. The intensity of peak reduction in Curve c

shows the affirmed attachment of PPyNTs to the AGA structure.

3.2 | Antimicrobial efficacy

We evaluated the MIC of PPyNT@AGA composite against gram-positive bacteria (*S. aureus* and *S. pneumonia*), gram-negative bacteria (*K. pneumonia*, *S. typhi*, and *P. aeruginosa*) and a fungal strain (*C. albicans*) by broth dilution assay. The corresponding absorbance at $\text{OD}_{600\text{ nm}}$ was observed and plotted in Figure 7. The MIC value for PPyNT@AGA against microbial pathogens was observed at $80\text{ }\mu\text{g/ml}$ concentration. It revealed a decrease in the absorption of the assay upon an increase in the concentration of PPyNT@AGA; no absorption was observed at a high concentration ($100\text{ }\mu\text{g/ml}$).

The antimicrobial activity of GA, AGA, PPyNTs and PPyNT@AGA were examined against gram-positive bacteria (*S. aureus* and *S. pneumonia*), gram-negative bacteria (*K. pneumonia*, *S. typhi*, and *P. aeruginosa*) and a fungal strain (*C. albicans*) using azithromycin and fluconazole as positive controls (Figure 8b). The images of disc diffusion assay showed significant zones of clearance for AGA and no activity for GA. The amine functionalised hybrid materials exhibited superior antimicrobial and antibiofilm activities against planktonic bacterial cells [39]. In AGA, the amine functional groups initiated cell attachment towards microbes and proved to be an inhibiting material with antimicrobial properties. The highest

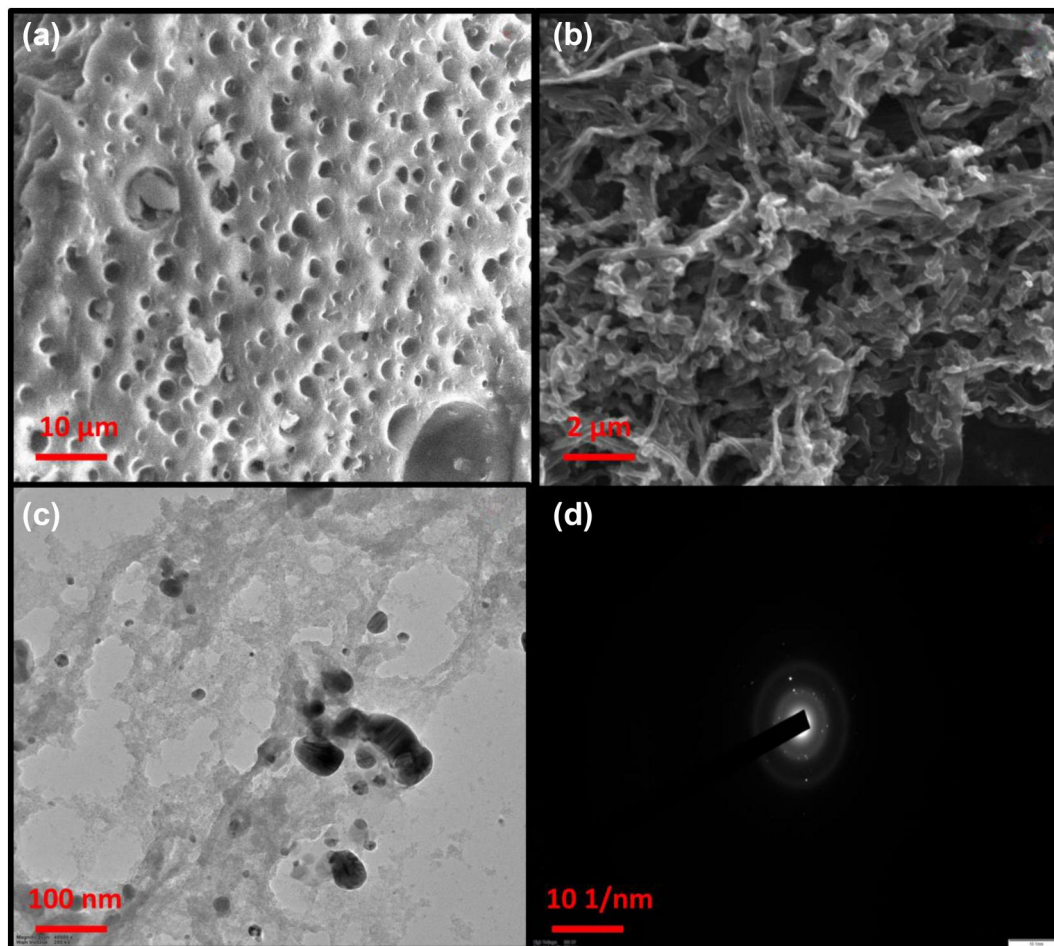


FIGURE 4 Field emission-scanning electron microscopy images of (a) aminated gum acacia, (b) polypyrrole nanotube-enhanced aminated gum acacia. Transmission electron microscopy image of (c) polypyrrole nanotube-enhanced aminated gum acacia and (d) SAED pattern. SAED, selected area electron diffraction

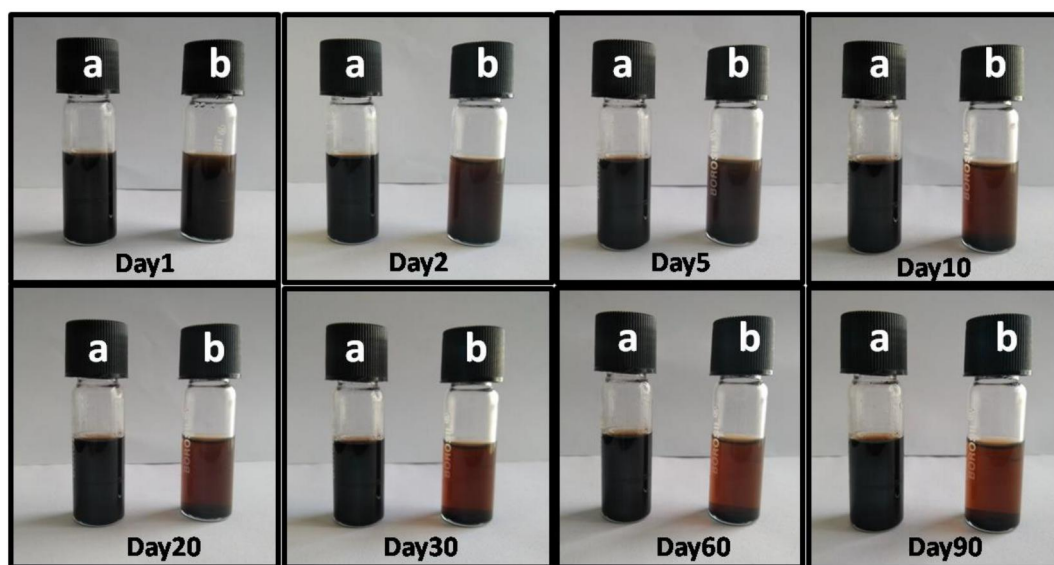


FIGURE 5 Photographs of polypyrrole nanotubes taken periodically: (a) with and (b) without aminated gum acacia dispersed solution in deionised water

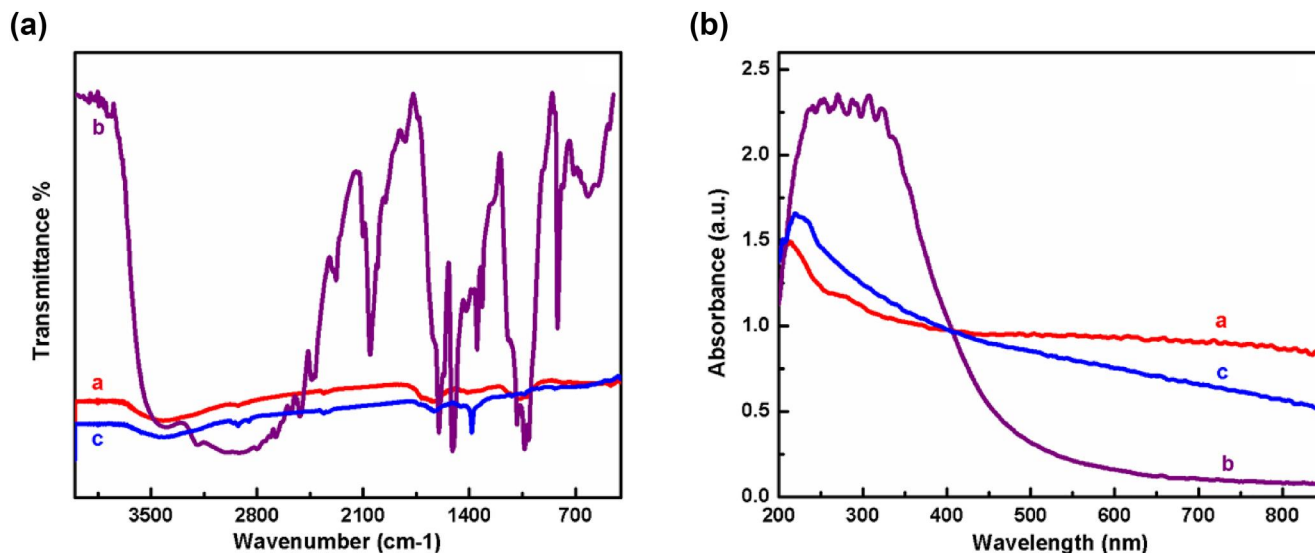


FIGURE 6 (a) Fourier transform-infrared spectrum and (b) UV-vis spectra of (a) polypyrrole nanotubes, (b) aminated gum acacia, (c) polypyrrole nanotube-enhanced aminated gum acacia nanocomposite

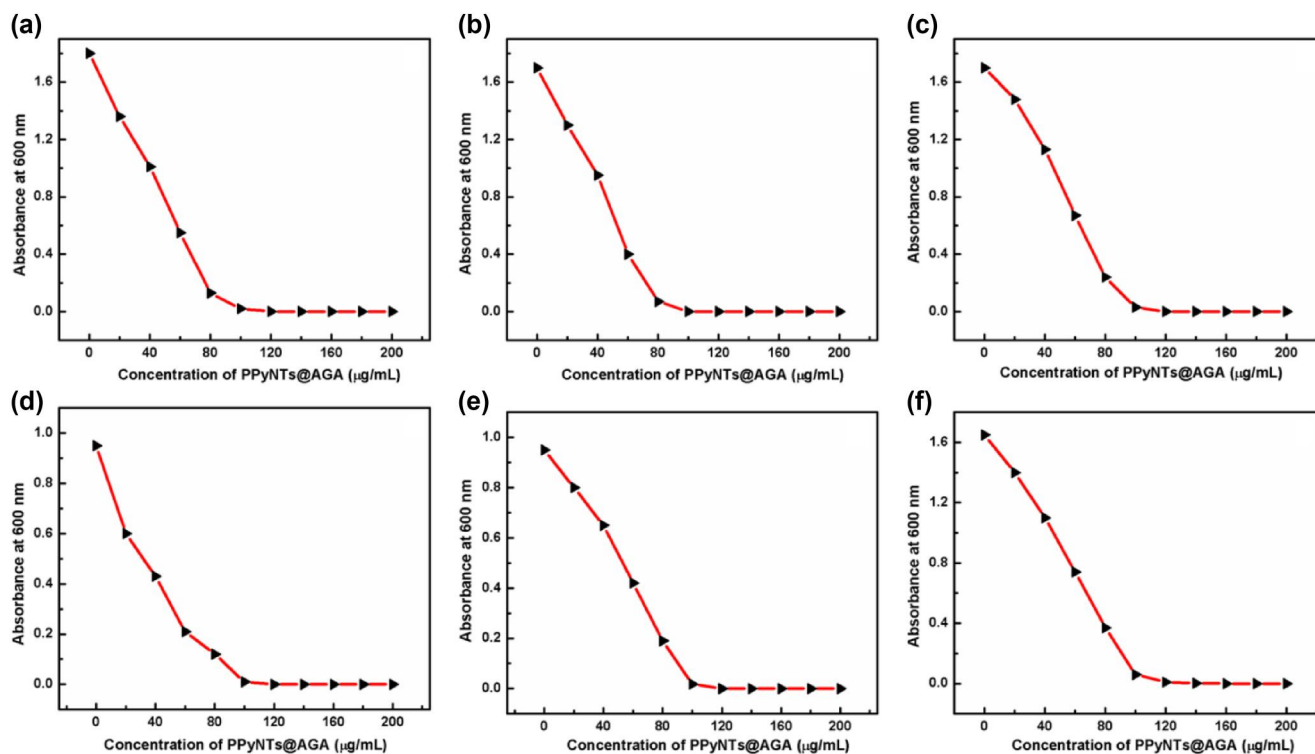


FIGURE 7 Microbial inhibitory concentration of polypyrrole nanotube-enhanced aminated gum acacia (0, 20, 40, 60, 80, 100, 120, 140, 160, 180 and 200 μg/ml) against (a) *S. aureus*, (b) *S. pneumoniae*, (c) *K. pneumoniae*, (d) *S. typhi*, (e) *P. aeruginosa* and (f) *C. albicans*

inhibition activity was observed in 20 μg/ml PPyNT@AGA against *S. aureus*, *S. pneumoniae*, *K. pneumoniae*, *S. typhi*, *P. aeruginosa* and *C. albicans*, and the corresponding zones of inhibition were 13, 11, 15, 12, 14 and 24 mm, respectively. The results clearly displayed an increased zone of clearance at the PPyNT@AGA composite compared with individual samples. The zone of clearance (in mm) of each plate was measured and presented as a bar graph (Figure 8a). Therefore, the prepared

PPyNT@AGA nanocomposite showed better antimicrobial efficacy.

Also, the PPyNT@AGA nanocomposite showed higher antimicrobial efficacy against gram-positive bacteria (*S. aureus* and *S. pneumoniae*), gram-negative bacteria (*K. pneumoniae*, *S. typhi*, and *P. aeruginosa*) and a fungal strain (*C. albicans*) compared with positive controls azithromycin and fluconazole (Figure 9) at varying concentrations. Antimicrobial growth

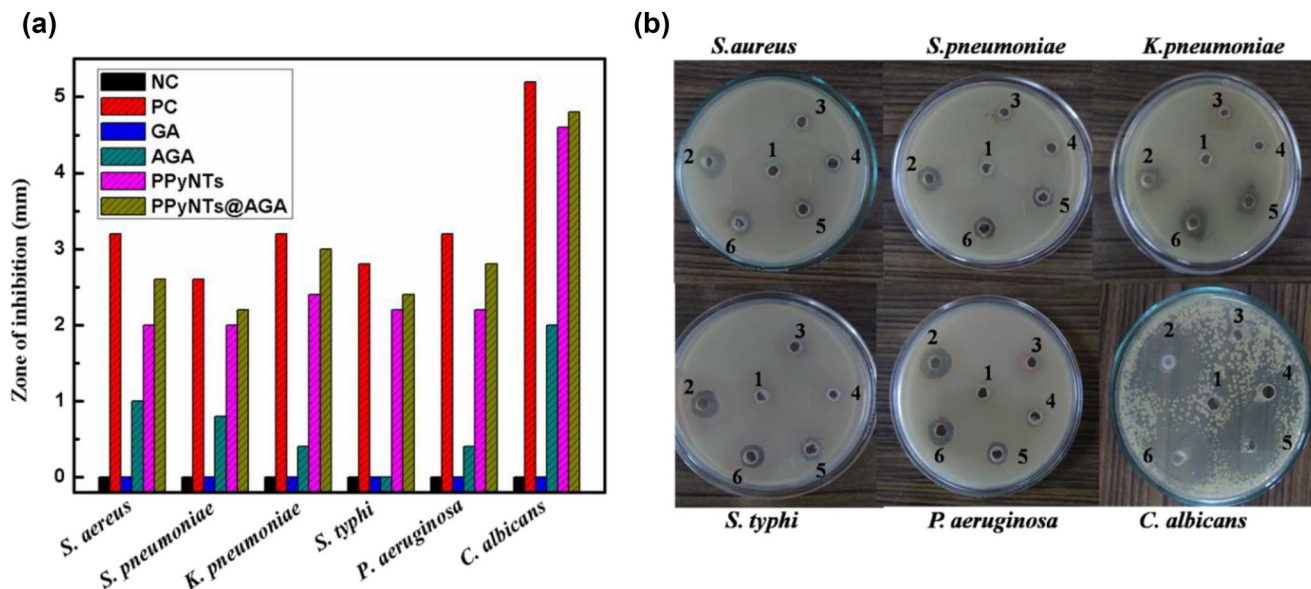


FIGURE 8 Antimicrobial activity (a) zone of inhibition and (b) zone of clearance for 20 $\mu\text{g/ml}$ of (1) negative control, (2) positive control, (3) gum acacia, (4) aminated gum acacia, (5) polypyrrole nanotubes, (6) polypyrrole nanotube-enhanced aminated gum acacia against different microbial pathogens

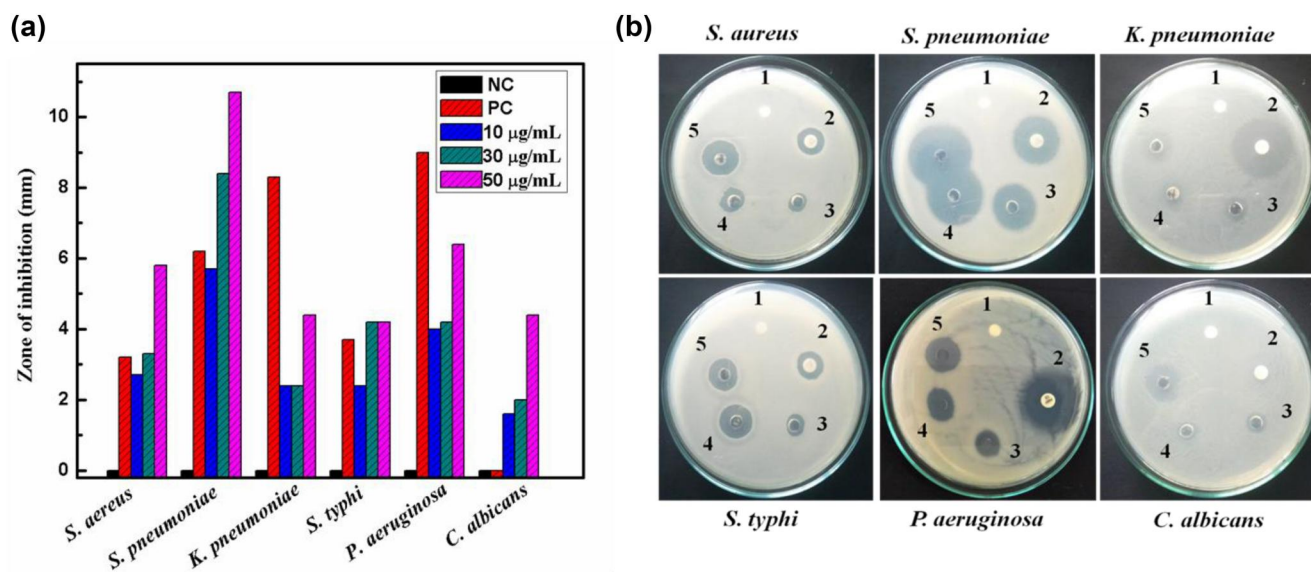


FIGURE 9 Antimicrobial activity of polypyrrole nanotube-enhanced aminated gum acacia composite: (a) Zone of inhibition and (b) zone of clearance using (1) 20 $\mu\text{g/ml}$ negative control; (2) 20 $\mu\text{g/ml}$ positive control at different concentrations; (3) 10 $\mu\text{g/ml}$; (4) 30 $\mu\text{g/ml}$; (5) 50 $\mu\text{g/ml}$ of polypyrrole nanotube-enhanced aminated gum acacia sample against different microbial pathogens

curve activity of the PPyNT@AGA composite was evaluated periodically (1–24 h) in different concentrations (10, 30, 50 and 100 $\mu\text{g/ml}$). Figure 10 shows the gradual inhibition of microbes encountering conditions of different concentrations with increasing time of interaction; it achieved stationary phase growth at 24 h. Kora et al. [40] explored the stability of silver NPs with rhamnolacturonan gum against gram-positive *S. aureus* and gram-negative *Escherichia coli* strains; they evaluated the time kinetics on the microbial growth and attained stationary phase at 48 h. Here, the proposed

PPyNT@AGA nanocomposite exhibited enhanced growth inhibition at 24 h and further affirmed stability against microbes. The mechanism of electrostatic interaction between the polycationic structure and the predominantly anionic components of the microorganisms have a pivotal role in antibacterial activity [41]. Thus, the negatively charged surface of the microbial cell is the target site for the positively charged groups in the PPyNT@AGA composite leading to leakage of intracellular components that cause cell damage. The number of ammonium groups linking to the polymer backbone of

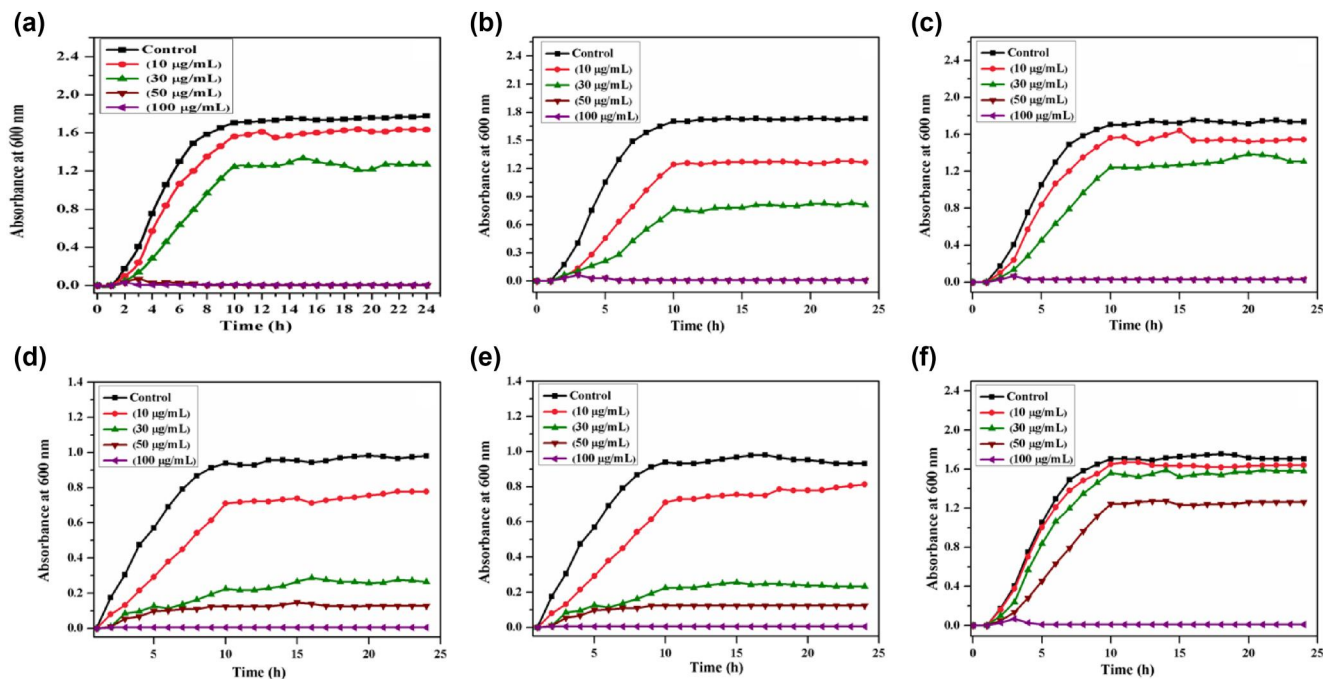


FIGURE 10 Growth kinetics of polypyrrole nanotube-enhanced aminated gum acacia composite at different concentrations (10, 30, 50 and 100 $\mu\text{g/ml}$), (negative control dimethyl sulfoxide, positive control azithromycin [bacteria], fluconazole [fungal]) against (a) *S. aureus*, (b) *S. pneumoniae*, (c) *K. pneumoniae*, (d) *S. typhi*, (e) *P. aeruginosa*, and (f) *C. albicans* for 24 h

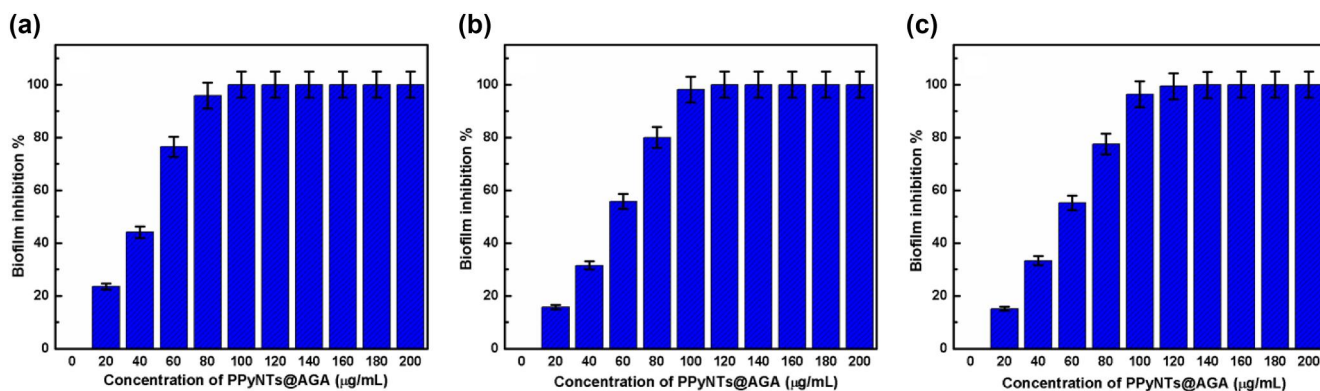


FIGURE 11 Effect of polypyrrole nanotube-enhanced aminated gum acacia on biofilm formation. The bar graph indicates the percentage of biofilm inhibition against (a) *S. pneumoniae*, (b) *P. aeruginosa* and (c) *C. albicans*

PPyNT@AGA was also substantially increased by amine modification of the GA structure, initiating good antimicrobial efficacy because of minimal cytotoxicity.

3.3 | Action of PPyNT-enhanced AGA nanocomposite on biofilm formation

The crystal violet quantification of biofilm formed in the absence and presence of increasing concentrations of a PPyNT@AGA composite (20–200 $\mu\text{g/ml}$) exhibited proportionally increased percentage of biofilm inhibition (Figure 11). The maximum biofilm inhibition of 96% was achieved for 100 $\mu\text{g/ml}$ PPyNT@AGA against gram-positive bacteria

(*S. pneumoniae*), gram-negative bacteria (*P. aeruginosa*) and a fungal strain (*C. albicans*). Hence, 100 $\mu\text{g/ml}$ of PPyNT@AGA was determined to be the biofilm inhibitory concentration and was taken for further assays.

The antibiofilm activity of GA and AGA were evaluated and are shown in Figures S2 and S3. Generally, GA, which is known to be potent against microbial pathogens, is used only as a stabilising agent for NPs in antimicrobial application [42]. However, here we found significant biofilm inhibition in AGA and speculated that the amine modification of GA is responsible for the cell attachment and disruption of microbial pathogens. The antibiofilm of AGA, PPyNTs and PPyNT@AGA against gram-positive bacteria (*S. pneumoniae*), gram-negative bacteria (*P. aeruginosa*) and the fungal strain

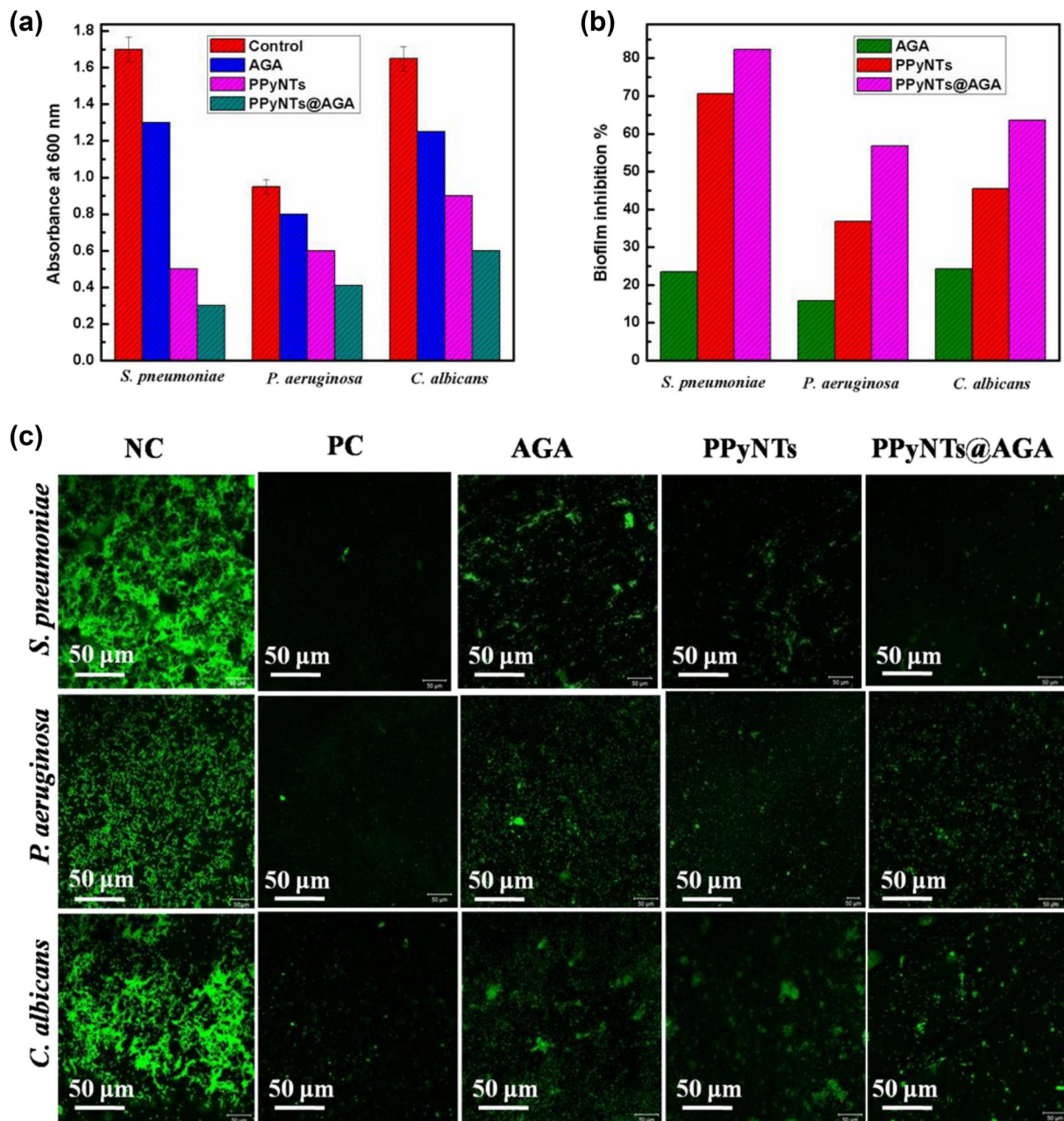


FIGURE 12 Biofilm inhibitory effect of 100 µg/ml aminated gum acacia, 100 µg/ml polypyrrole nanotubes and 100 µg/ml polypyrrole nanotube-enhanced aminated gum acacia incubated at 37°C for 24 h in (a) OD600 nm graph, (b) Biofilm inhibition % (c) confocal laser scanning microscopy (CLSM) images of maturely formed microbial biofilm with negative control (NC) (20 µg/ml dimethyl sulfoxide), positive control (PC) (20 µg/ml azithromycin for bacteria and 20 µg/ml fluconazole for fungi). In the CLSM image, living microbes emit green light and no colour for dead cells

(*C. albicans*) incubated at 37°C for 24 h was efficacious (Figure 12). After 24 h of incubation, the PPyNT@AGA showed higher antibiofilm activity than PPyNTs or AGA.

We evaluated the antibiofilm activity of PPyNT@AGA nanobiocomposite against microbes such as *S. pneumoniae*, *P. aeruginosa*, and *C. albicans*. From the interaction of microbes with PPyNTs/AGA composite for 24 h, it is found that the biofilm formation ability is decreased with increasing composite concentration (Figure 13). Thus, more than 90% biofilm inhibition was observed at 50 µg ml⁻¹ concentrations and 85% at 30 µg ml⁻¹. Also the lowest MIC value (10 µg ml⁻¹) showed

prominent antibiofilm activity. In addition, the control DMSO and water had no significant biofilm inhibition activity. The positive control fluconazole exhibited more biofilm inhibition activity. These data indicate that the PPyNT@AGA composite impedes biofilm formation by *P. aeruginosa*, *S. pneumoniae* and *C. albicans*. The impeding mechanism may repress the protein in microbial pathogens, resulting in damage to the exopolymeric matrix, leading to cell death [37]. Sun et al. [43] reported the mechanism of antibiofilm efficacy of positively charged glycine modified lipid NPs against microbial pathogens. The maximum biofilm inhibition was found in the case

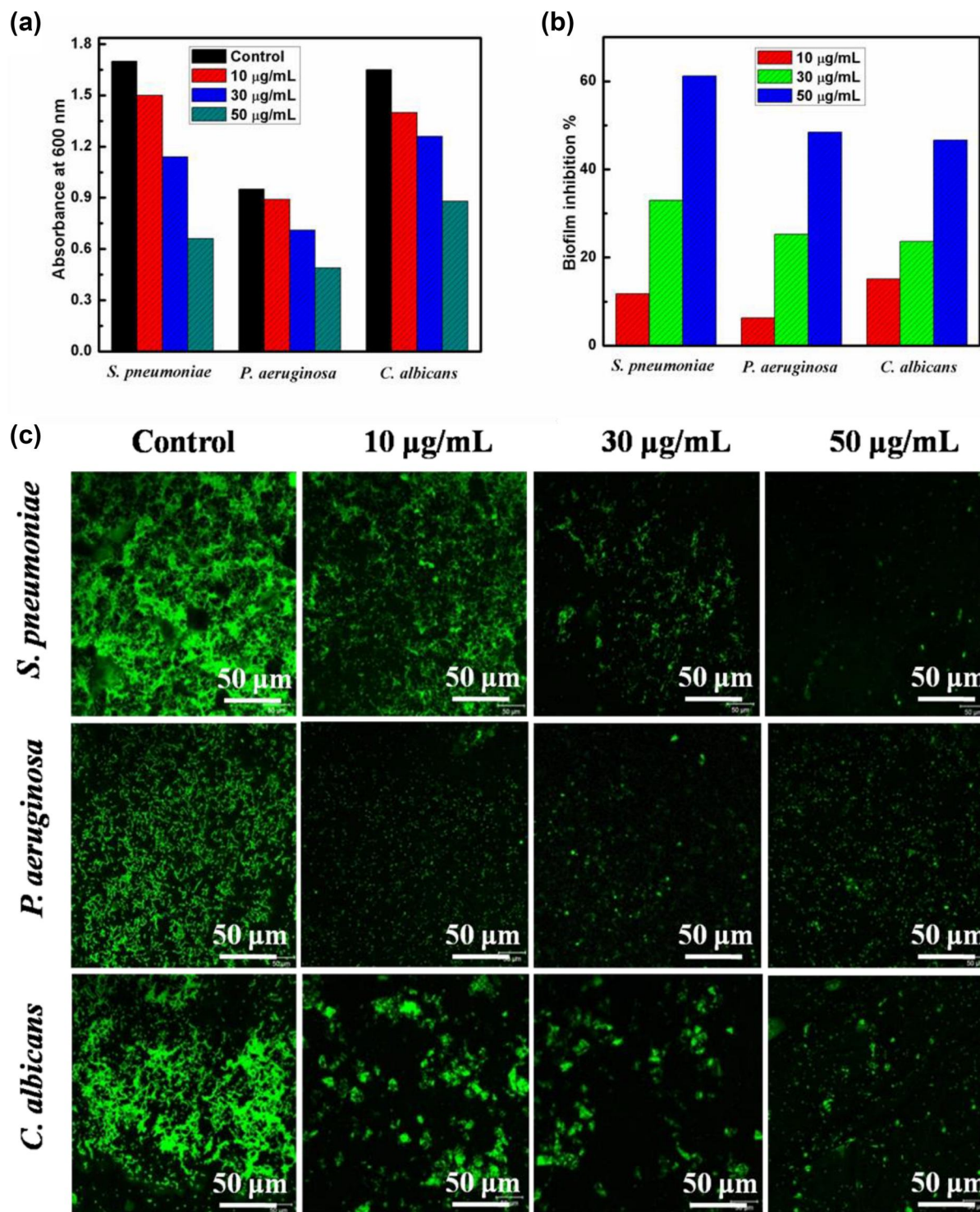


FIGURE 13 Biofilm inhibitory effect of polypyrrole nanotube-enhanced aminated gum acacia at varying concentrations of 10, 30, and 50 µg/ml incubated at 37°C for 24 h in (a) OD600 nm graph (b) Biofilm inhibition % (c) confocal laser scanning microscopy (CLSM) images of maturely formed microbial biofilm after contact. In the CLSM image, living microbes emit green light and no colour for dead cells studies

of the PPyNT@AGA nanocomposite owing to the strong interaction of N^+ in amine-modified GA and PPyNTs towards the negatively charged cell membrane of microbes. Hence, it was speculated that the disruption in cell membranes of microbial pathogens eventually caused a decrease in cell

metabolism and resulted in microbial pathogen die-off. Thus, the facile interaction of positively charged PPyNT@AGA towards microbial cell membrane caused the accumulation of more positive charges and demonstrated good antibiofilm efficacy. In previously reported studies, antimicrobial and

antibiofilm efficacy were demonstrated using GA and NPs with better inhibition activity [11, 44]. For example, 125 $\mu\text{g}/\text{ml}$ of ZnO/GA-based composite showed 85% of inhibition against *S. aureus* and exhibited MIC antibiofilm activity at a concentration of 500 $\mu\text{g}/\text{ml}$ [42]. Here, the PPyNT@AGA nanocomposite had better antimicrobial and antibiofilm studies at different concentrations. Notably, 100 $\mu\text{g}/\text{ml}$ of PPyNT@AGA inhibited 94.11% of *S. pneumoniae*, 95.78% of *P. aeruginosa* and 90.90% of *C. albicans*. Therefore, the proposed nanocomposite showed enhanced antibiofilm activity against gram-positive bacteria (*S. pneumoniae*), gram-negative bacteria (*P. aeruginosa*) and a fungal strain (*C. albicans*).

4 | CONCLUSIONS

We developed a sol-gel based approach to prepare a PPyNT-embedded AGA-based nanocomposite for antibiofilm and antimicrobial applications. The physicochemical property of the PPyNT@AGA composite is greatly enhanced by the electrosteric stabilisation effect of AGA, which in turn exhibited a more agglomeration-free, highly soluble and dispersible composite. As a result, strongly binding and accumulated cationic active sites in the as-prepared nanocomposite are extensively attached towards the cell wall of microbial pathogens. The antimicrobial and antibiofilm studies of PPyNT@AGA also revealed higher antimicrobial and antibiofilm efficacy and thus proved it to be a better biocompatible platform for future applications such as drug delivery and pharmaceutical and food industries. The long-term antimicrobial ability of the sample demonstrated its powerful role as an antimicrobial agent, which makes it a template for a design in wearable biomedical applications.

ORCID

Nathiya Dhananjayan  <https://orcid.org/0000-0001-6011-4008>

Wilson Jeyaraj  <https://orcid.org/0000-0002-2260-4986>

REFERENCES

- Li, X.-G., et al.: Efficient and scalable synthesis of pure polypyrrole nanoparticles applicable for advanced nanocomposites and carbon nanoparticles. *J. Phys. Chem. C.* 114(45), 19244–19255 (2010)
- Khan, F., et al.: Antibiofilm and antivirulence properties of chitosan-polypyrrole nanocomposites to *Pseudomonas aeruginosa*. *Microb. Pathog.* 128, 363–373 (2019)
- Da Silva Jr., F.G., et al.: Antibacterial behaviour of polypyrrole: the influence of morphology and additives incorporation. *Mater. Sci. Eng. C.* 62, 317–322 (2016)
- Zhou, S., et al.: Facile template synthesis of microfibrillated cellulose/polypyrrole/silver nanoparticles hybrid aerogels with electrical conductive and pressure responsive properties. *ACS Sustainable Chem. Eng.* 3(12), 3346–3354 (2015)
- Zhang, S., et al.: UV-catalytic preparation of polypyrrole nanoparticles induced by H_2O_2 . *J. Phys. Chem. C.* 2015, 119, (32), 18707–18718
- Liu, P., Wang, X., Wang, Y.: Design of carbon black/polypyrrole composite hollow nanospheres and performance evaluation as electrode materials for supercapacitors. *ACS Sustainable Chem. Eng.* 2(7), 1795–1801 (2014)
- Vetter, C.A. et al.: Novel synthesis of stable polypyrrole nanospheres using ozone. *Langmuir.* 27(22), 13719–13728 (2011)
- Zhang, X., et al.: Controllable synthesis of conducting polypyrrole nanostructures. *J. Phys. Chem. B.* 110(3), 1158–1165 (2006)
- Jang, J., Yoon, H.: Formation mechanism of conducting polypyrrole nanotubes in reverse micelle systems. *Langmuir.* 21(24), 11484–11489 (2005)
- Murugesan, B., et al.: Fabrication of palladium nanoparticles anchored polypyrrole functionalised reduced graphene oxide nanocomposite for antibiofilm associated orthopaedic tissue engineering. *Appl. Surf. Sci.* 510, 145403 (2020)
- Murugesan, B., et al.: Highly biological active antibiofilm, anticancer and osteoblast adhesion efficacy from MWCNT/PPy/Pd nanocomposite. *Appl. Surf. Sci.* 434, 400–411 (2018)
- Maruthapandi, M., et al.: Carbon-dot initiated synthesis of polypyrrole and polypyrrole@CuO micro/nanoparticles with enhanced antibacterial activity. *ACS Appl. Polym. Mater.* 1(5), 1181–1186 (2019)
- Tavousi, A., Ahmadi, S., Zohrabi, P.: Polypyrrole-modified magnetic nanoparticles and high-performance liquid chromatography for determination of glibenclamide from biological fluids. *IET Nanobiotechnol.* 13(5), 47–53 (2019)
- Liu, F., et al.: Synthesis of polypyrrole nanocomposites decorated with silver nanoparticles with electrocatalysis and antibacterial property. *Compos. B. Eng.* 69, 232–236 (2015)
- Wan, C., Li, J.: Cellulose aerogels functionalised with polypyrrole and silver nanoparticles: in-situ synthesis, characterisation and antibacterial activity. *Carbohydr. Polym.* 146, 362–367 (2016)
- Manivasagan, P., et al.: Multifunctional biocompatible chitosan-polypyrrole nanocomposites as novel agents for photoacoustic imaging-guided photothermal ablation of cancer. *Sci Rep.* 7, 43593 (2017)
- Bideau, B., et al.: Mechanical and antibacterial properties of a nanocellulose-polypyrrole multilayer composite. *Mater. Sci. Eng. C.* 69, 977–984 (2016)
- Weinbreck, F., et al.: Complex coacervation of whey proteins and gum Arabic. *Biomacromolecules.* 4(2), 293–303 (2003)
- Zare, E.N., et al.: Antimicrobial gum bio-based nanocomposites and their industrial and biomedical applications. *Chem. Commun.* 55(99), 14871–14885 (2019)
- Amalraj, A., et al.: Preparation, characterisation and antimicrobial activity of polyvinyl alcohol/gum Arabic/chitosan composite films incorporated with black pepper essential oil and ginger essential oil. *Int. J. Biol. Macromol.* 151, 366–375 (2020)
- Bandyopadhyaya, R., et al.: Stabilisation of individual carbon nanotubes in aqueous solutions. *Nano. Lett.* 2(1), 25–28 (2002)
- Nishi, K.K., Antony, M., Jayakrishnan, A.: Synthesis and evaluation of ampicillin-conjugated gum Arabic microspheres for sustained release. *J. Pharm. Pharmacol.* 59(4), 485–493 (2007)
- Valliammai, A., et al.: 5-Dodecanolide interferes with biofilm formation and reduces the virulence of Methicillin-resistant *Staphylococcus aureus* (MRSA) through up regulation of agr system. *Sci. Rep.* 9(1), 1–16 (2019)
- Maráková, N., et al.: Antimicrobial activity and cytotoxicity of cotton fabric coated with conducting polymers, polyaniline or polypyrrole, and with deposited silver nanoparticles. *Appl. Surf. Sci.* 396, 169–176 (2017)
- Khan, A.A.P., et al.: Sensor development of 1,2 Dichlorobenzene based on polypyrrole/Cu-doped ZnO (PPY/CZO) nanocomposite embedded silver electrode and their antimicrobial studies. *Int. J. Biol. Macromol.* 98, 256–267 (2017)
- Zhao, R., et al.: Stable nanocomposite based on PEGylated and silver nanoparticles loaded graphene oxide for long-term antibacterial activity. *ACS Appl. Mater. Interfaces.* 9(18), 15328–15341 (2017)
- Ren, J.M., et al.: Star polymers. *Chem. Rev.* 116(12), 6743–6836 (2016)
- Radhakrishnan, S., et al.: Polypyrrole nanotubes-polyaniline composite for DNA detection using methylene blue as intercalator. *Anal. Methods.* 5(4), 1010–1015 (2013)
- Dhananjayan, N., Jeyaraj, W., Karuppasamy, G.: Interactive studies on synthetic nanopolymer decorated with edible biopolymer and its selective electrochemical determination of L-tyrosine. *Sci. Rep.* 9(1), 13287 (2019)

30. Gowrishankar, S., Duncun Mosioma, N., Karutha Pandian, S.: Coral-associated bacteria as a promising antibiofilm agent against methicillin-resistant and-susceptible *Staphylococcus aureus* biofilms. *Evid-Based Complement. Altern. Med.* 2012 (2012)
31. Prasath, K.G., et al.: Palmitic acid inhibits the virulence factors of *Candida tropicalis*: biofilms, cell surface hydrophobicity, ergosterol biosynthesis, and enzymatic activity. *Front. Microbiol.* 11, 864 (2020)
32. CLSI (2017). Reference method for broth dilution antifungal susceptibility testing of yeasts— fourth edition: M27. Wayne, PA: Clinical and Laboratory Standards Institute. <https://doi.org/10.1093/cid/cis697>
33. Sarker, S.D., Nahar, L., Kumarasamy, Y.: Microtitre plate-based antibacterial assay incorporating resazurin as an indicator of cell growth, and its application in the in vitro antibacterial screening of phytochemicals. *Methods.* 42(4), 321–324 (2007)
34. Nallasamy, P., et al.: Polyherbal drug loaded starch nanoparticles as promising drug delivery system: antimicrobial, antibiofilm and neuro-protective studies. *Process. Biochem.* 92, 355–364 (2020)
35. Yeroslavsky, G., et al.: Sonochemically-produced metal-containing polydopamine nanoparticles and their antibacterial and antibiofilm activity. *Langmuir.* 32(20), 5201–5212 (2016)
36. Nathiya, D., et al.: Stable and robust nanobiocomposite preparation using aminated guar gum (mimic activity of graphene) with electron beam irradiated polypyrrole and Ce-Ni bimetal: effective role in simultaneous sensing of environmental pollutants and pseudocapacitor applications. *Electrochim. Acta.* 246, 484–496 (2017)
37. Hong, Y.K., et al.: Effects of electron-beam irradiation on conducting polypyrrole nanowires. *Appl. Phys. Lett.* 94(5), 053111 (2009)
38. Williams, D.N., et al.: Surface modification of magnetic nanoparticles using gum Arabic. *J. Nanopart. Res.* 8(5), 749–753 (2006)
39. Zarafu, I., et al.: Antimicrobial features of organic functionalised graphene-oxide with selected amines. *Materials.* 11(9), 1704 (2018)
40. Kora, A.J., Sashidhar, R.B.: Biogenic silver nanoparticles synthesised with rhamnolacturonan gum: antibacterial activity, cytotoxicity and its mode of action. *Arabian J. Chem.* 11(3), 313–323 (2018)
41. Cheow, W.S., Hadinoto, K.: Lipid-polymer hybrid nanoparticles with rhamnolipid-triggered release capabilities as anti-biofilm drug delivery vehicles. *Particuology.* 10(3), 327–333 (2012)
42. Pauzi, N., Zain, N.M., Yusof, N.A.A.: Gum Arabic as natural stabilising agent in green synthesis of ZnO nanofluids for antibacterial application. *J. Environ. Chem. Eng.* 8(3), 103331 (2020)
43. Sun, L.m., Zhang, C.l., Li, P.: Characterisation, antibiofilm, and mechanism of action of novel PEG-stabilised lipid nanoparticles loaded with terpinen-4-ol. *J. Agric. Food Chem.* 60(24), 6150–6156 (2012)
44. Sharma, S., et al.: Preparation of gum acacia-poly(acrylamide-IPN-acrylic acid) based nanocomposite hydrogels via polymerisation methods for antimicrobial applications. *J. Mol. Struct.* 1215, 128298 (2020)

SUPPORTING INFORMATION

Additional supporting information may be found online in the Supporting Information section at the end of this article.

How to cite this article: Dhananjayan N, Viswanathan K, Jeyaraj W, Ayyakannu A, Karuppasamy G. Antibiofilm and antimicrobial efficacy evaluation of polypyrrole nanotubes embedded in aminated gum acacia based nanocomposite. *IET Nanobiotechnol.* 2021;15:441–454. <https://doi.org/10.1049/nbt2.12055>